Bas-reliefs modelling based on learning deformable 3D models

Siyuan Zhu
College of Information Engineering
Northwest A & F University
Yangling, China
2017050988@nwsuaf.edu.cn

Cheng Shang
College of Information Engineering
Northwest A & F University
Yangling, China
anshidiandu@foxmail.com

Jingjing Fan
College of Information Engineering
Northwest A & F University
Yangling, China
254453700@qq.com

Xin Wang
College of Information Engineering
Northwest A & F University
Yangling, China
1074976393@ qq.com

Meili Wang*
College of Information Engineering
Northwest A & F University
Yangling, China
wml @nwsuaf.edu.cn

***Abstract*—Bas-relief is a special art-form, which can be used as decorations. Deformable 3D models are usually used in image segmentation and 3D reconstruction, aiming at the reconstruction of certain category especially. To quickly reconstruct different objects of the same category and take the psychological process and visual characteristics of human observation images into account, in this paper, we propose a bas-reliefs generation method for flowers based on deformable 3D models which is a type of parametric model that can deform shapes by changing related parameters. First, we create a dataset by labelling images with keypoints. Then, we use Non Rigid Structure from Motion (NRSfM) algorithm to estimate viewpoints. A deformable 3D model is reconstructed by Visual Hull. Next, we deform the 3D model to a variant of the object according to an input 2D image. After that, we enhance and smoothen the image by applying gamma correction on the gray scale image with gradient. Finally, we calculate height values as details using illumination model and add them to the variant. The experimental results demonstrate that our method can reconstruct bas-reliefs for flowers in different shapes with complex background, which is also proven to be able to extend to other categories, such as birds and fishes.**

Keywords—bas-relief, deformable 3D models, detail extraction

I. INTRODUCTION

Relief is usually carved on a base surface, which is a special art form in-between sculpture and drawing. Zhang et al. [1] provided an overview of their art characteristics. According to its depth, relief can be categorized into three groups generally: high relief, bas-relief and sunken relief. Bas-relief is one of the most representative art forms with a long history since it can represent an object with a limited height [2]. The bas-relief productions can be regarded as artworks themselves or as decorations to decorate furniture, walls and so on [3]. Flower bas-reliefs are commonly used as decorations in our life as shown in Fig.1.

(a) wall hanging (b) fresco (c) vase

Fig. 1. The application of flower bas-reliefs as decorations.

Traditional relief is handmade by artists which not only requires professional skills but also is laborious and time consuming. The techniques of digital relief generation integrate computer science technology into artistic creation, which provides the convenience of relief generation and possibilities of massive scale production. Currently, the techniques of digital relief generation can be categorized into image based and 3D model based. Image-based method is easier than model-based method due to the large amount of available data, hence there are more researches about image-based relief generations, which can be further categorized into three areas: methods based on RGB image [4, 5] , normal map [6-8] and depth map [6] , while our method belongs to the first kind.

In this paper, flower bas-relief is the main concern of our study. According to the deformability of 3D models, we reconstruct a variant of the corresponding flower, and then extract the detail from the image using gray level information and add it to the variant. The result of this work can provide the convenience of relief generation and possibilities of massive scale production. The contributions of this paper are as follows:

- A novel method to generate flower bas-reliefs with different number of petals is presented, and we extend the method to other categories.
- A detail extraction method with image enhancement is implemented based on different images. The results are

Key Laboratory of Agricultural Internet of Things, Ministry of Agriculture and Rural Affairs, Yangling, Shaanxi 712100, China(2018AIOT-09), National Natural Science Foundation of China(61702433), Key Research and Development Programm of Shaanxi province(2018NY-127).

*Corresponding author: Meili Wang Email: wml @nwsuaf.edu.cn

978-1-7281-6926-2/20/$31.00 ©2020 IEEE

added on the shapes of bas-reliefs, and we achieve realistic bas-relief models.

The rest of the paper is organized as follows: Section 2 reviews related works on bas-relief generation, deformable 3D models and details extraction. Section 3 describes our method in detail. Section 4 shows the experimental results and analysis. Section 5 gives the conclusions and suggestions of future works.

II. Related works

A. Bas-relief generation

Bas-relief generation methods can be categorized into image based and 3D model based. Wang et al. [3] reviewed the technologies of model-based digital relief generation. As for the methods of image-based relief generation, they mainly use feature extraction, 3D reconstruction technologies to transform a 2D image to a 3D relief [3].

Depth information is often needed in 3D reconstruction. Zeng et al. [4] proposed an approach using region extraction and depth relationship inference to generating bas-reliefs from a single image. Sohn [5] computed a depth map from a set of photographs, and constructed a detail map using pixel values of the input image. Dvorožňák et al. [6] separated the object into a set of semantically meaningful parts. Then they inflated individual component until it has a semi-elliptical profile, and connected them seamlessly. However, relative depth order must be known beforehand. Lu et al. [7] compressed the height field to generate the base mesh of bas-relief. Then they used the intensity images to extract the information of gray level, gradient and saliency. Finally, they added gray and gradient information into the height field of base mesh of relief to preserve the facial details. The disadvantage of that method was that, poor capturing equipment may affect experimental results, and it was also needed to remove the highlights from the color image by hand. Normal maps can reflect the changes of the surface detail fully and avoid the discontinuity of the height field caused by occlusion. Ji et. al [8-10] had paid attention to normal maps in relief generation. In [9] they used a GPU-based acceleration method, which took advantage of depth-and-normal maps to generate bas-relief. And in [10] they developed decomposition-and-composition operations on normal maps and edited the normal image in a layer-based way to get different appearances of the resulted bas-reliefs. Ultimately, they generated bas-reliefs from a single RGB image and its edge-based sketch image. While Wei et al. [2] decomposed the normal field into a piecewise smooth base layer and a detail layer.

On the other hand, some researchers started from the perspective of feature information in images. Meng et al. [11] has estimated metric depth of relief model by Shape from Shading (SFS), and restored it by using transformation and model superposition. Wu and Liu [12] extracted the height field according to the gray value, and then enhanced and superimposed the details. But there were still some problems in the algorithm, such as how to extract high quality details better. Lee and Sohn [13] proposed a method to generate a cartoon-style bas-relief surface by Non Photorealistic Rendering (NPR) and image processing technology. To and Sohn [14] detected and protruded the facial features by adjusting the brightness valued of the area. Their results proved that it could resolve the problem of generating erroneous 3D depth. Zhu et al. [15] proposed an overlay based bas-relief generation algorithm, aiming at the problem of the detail features of bas-relief generated by image and the relative position of the features in the bas-relief space.

In addition, there are some limitations in image-based relief generation, it could only achieve a better result in fields like face reliefs [7] , Chinese calligraphy reliefs [16] , brick reliefs [17] and so on. Zhang et al. [16] used Laplacian-based mesh inflations to convert the 2D fonts into the form of a 2.5D relief. Then combined homogeneous and inhomogeneous height fields facilitates shape manipulation. Li et al. [17] estimated the base relief of the low frequency component with a Partial Differential Equation (PDE) - based mesh deformation scheme automatically. And the high frequency detail was estimated directly from rubbing images automatically or optionally with minimal interactive processing. Although they could obtained bas-relief from certain field, they did not extend to other objects. That is what this paper aims to do.

B. Deformable 3D models

The deformable 3D model is a parameterized triangular elastic mesh, and the vertex of the triangle is the vertex of the deformable 3D model. Since Terzopoulos, Witkin and Kass [18, 19] first applied deformable 3D models to surface reconstruction, the deformable 3D model has been widely used in image segmentation and surface reconstruction [20]. Deformable 3D models based technology provides a new idea for effectively segmenting and reconstructing objects from images. Taking the psychological process and visual characteristics of human observation images into account, it is a top-down technology [21]. The basic idea is to establish the corresponding relationship between the images and the 3D representation of the same kind of objects using linear combination.

Hu [22] proposed a mesh resampling method, and constructed a multi-resolution model. It overcame the model matching problems in complex illumination. But it was time consuming. Shu et al. [23] took a single image as input. First, a sparse face model was reconstructed from an image using Sparse Morphable Model. Then a General Face Model was warped and the texture was synthesized. Finally the 3D model was caricatured. Prased et al. [24] extended contour-based reconstruction techniques, and reconstructed deformable 3D models of clown fish from unordered images. Hwang et al. [25] proposed a 3D face modelling method, which used multiple 3D deformable face models in a mirror system. Suwajanakorn et. al [26] presented a new dense 3D flow estimation method coupled with SFS. They derived a person-specific face model, and incorporated shading cues to obtain high resolution details. Kar et al. [27] learnt a deformable 3D model from available 2D annotations, and the dataset came from existing datasets of object detection. They complemented it with a bottom-up module for recovering high-frequency shape details. While Vicente et al. [28] reconstructed 3D models from a fully annotated image set. Feng et al. [29] matched a set of morphable models against the 3D scan to automatically rig a 3D mesh. In addition, they used a morphable model to reshape and resize the 3D scan in the light of approximate human proportions. We were inspired by the work of Kar et al. [27] but they mainly paid

attention to vehicles such as cars, airplanes and motorbikes. Moreover, they just reconstructed the shape of objects without details on it. What we are concerned about are the categories that are suitable for generating bas-reliefs with details.

C. Detail extraction

For detail extraction, there are some methods based on skeleton fusion filter [30] and improved balanced histogram [31]. They could extract details more correctly than ever before, but time consuming. Yang et al. [32] proposed an improved multi-scale surface representation and detail enhancement method, which realized the transfer of geometric details, space-time deformation and local details enhancement, but ignored the enhancement of edges. To and Sohn [14] enhanced details by detecting the facial features and making them protruded by adjusting the brightness values of the areas. Sohn [5] described a new method that generate bas-relief on smartphone by compositing a base map and a detail map. Xu et al. [33] generated simple details for bas-reliefs by solving Poisson equation. Zhu et al. [15] proposed an overlay based bas-relief generation algorithm, and obtained bas-reliefs on faces. They also carried experiments on flowers in relief with less details. We could take the law of Illumination Intensity in their method to recover coarse details and enrich them further.

III. Our Method

A. Data preparation

Firstly, we collect 171 flower images from the internet with 'single flower' as the search term, including 147 five-petal and 24 four-petal. After that we define and label 11 keypoints (petal1, petal2, petal3, petal4, petal5, bifurcation1, bifurcation2, bifurcation3, bifurcation4, bifurcation5, stamen) and contour points according to the structure of flowers. As for four-petal flowers which don't have 'petal5' and 'bifurcation5', we label their coordinates as 'NULL'.

As shown in Fig.2, where red crosses represent keypoints and yellow dots represent contour points. The relief model consists of basic shape and surface detail. In the next step, we apply Non Rigid Structure from Motion(NRSfM) algorithm in reference [27] to estimate the viewpoint and use Visual Hull algorithm to reconstruct the basic shape of deformable 3D model. And we optimize the deformation of the model under the estimated viewpoint.

Fig. 2. Label example.

B. Learn a flower deformable 3D model

1) NRSFM MODEL

The 2D image is obtained from the 3D scene by cameras, and the camera model is the abstract of the actual camera which reflects the relationship between the 3D points and 2D points. The keypoints of different images are equipped with different viewpoints. Once the viewpoints and camera parameters are calculated, we can lift 2D points to 3D points, and finally reconstruct the model. NRSfM [27] provides the method to recover the 3D structure of the deformation object from 2D image feature point sequences.

The annotated dataset $T:\{(O_n,K_n)\}_{n=1}^{N}$, where O_n is the silhouette and K_n denotes an observed matrix composed of the k ($k=11$ in flower dataset) annotated keypoints coordinates(x_n^i and y_n^i represent the coordinate values of x-axis and y-axis of i^{th} keypoints of n^{th} instance respectively). $n\in\{1,...,N\}$, N denotes the number of instances in dataset, and $N=171$ in flower dataset.

$$K_n=\begin{bmatrix} x_n^1 & \dots & x_n^k \\ y_n^1 & \dots & y_n^k \end{bmatrix} \tag{1}$$

K_n is assumed to be the projection under $\pi_n=(c_n, R_n, T_n)$ of the 3D shape W_n with white noise N_n. c_n represents the scale factor, R_n represents the rotation matrix, and T_n represents the translation vector. The objective of the solution is to infer the parameters $\{\overline{W}, V\}$, camera parameters (c_n, R_n, T_n) and deformation parameters $\{z_n\}$ for all shapes W_n. Our adaptation of the NRSfM algorithm in [27] corresponds to maximizing the likelihood of the following model:

$$\begin{aligned} &K_n = c_n R_n W_n + 1^T T_n + N_n \\ &W_n = \overline{W} + V z_n \\ &z_n \sim \mathrm{N}(0, I) \quad N_n \sim \mathrm{N}(0, \sigma^2 I) \\ &\text{subject to: } R_n R_n^T = I_2 \end{aligned} \tag{2}$$

$$\sum_{k=1}^{K} C_n^{mask}(p_k, n) = 0, \forall n \in \{1,...,N\} \tag{3}$$

Where the shape is parameterized as a factored Gaussian with a mean shape $\overline{W}$, deformation bases $V=[V_1, V_2,\dots V_k]$ and latent deformation parameters z_n. I_2 is a second-order unit matrix. C_n^{mask} denotes the Chamfer distance field of the n^{th} instance's binary mask and means that all keypoints of the variant should lie inside its binary mask.

2) DEFORMABLE 3D MODEL LEARNING

Visual Hull algorithm is a 3D reconstruction method based on contour of the object. Taking a sequence of flower images as input and the corresponding viewpoints obtained in the previous step, the Visual Hull algorithm can be used to reconstruct the deformable 3D models. The shape model

$M=(\bar{S},V)$ is comprised of a mean shape $\bar{S}$ and deformation bases $V=\{V_1,...,V_K\}$ learnt from dataset $T:\{(O_i,K_i)\}_{i=1}^{N}$. $\pi(S)$ is the 2D projection of shape S, $\Delta^k(a;B)$ is defined as the square average distance of point a to its k-nearest neighbors in set B. Deformation parameters are optimized based on silhouette consistency, keypoint consistency, deformation consistency and smoothness consistency [27], as shown in (4)-(8).

Silhouette Consistency. It enforces the predicted shape of an instance to project inside its silhouette achieved by penalizing the points project outside the instance mask by their distance from the silhouette and encourages points on the Silhouette to pull nearby projected points towards them. As shown in (4):

$$E_{sc}(S,O,\pi)=\sum_{C^{mask}(p)>0}\Delta^1(p;O)+\sum_{p\in O}\Delta^m(p;\pi(S)) \tag{4}$$

Keypoint Consistency. It is represented by the chamfer distance from the 3D keypoint W to the shape S. Limit the distance between the two can satisfy consistency.

$$E_{kp}(S,W)=\sum_{\kappa\in W}\Delta^m(\kappa;S) \tag{5}$$

Deformation Consistency. In addition to the above data terms, we use a simple shape regularizer to restrict arbitrary deformations by imposing a quadratic deformation penalty between each point and its neighbors. The parameter δ represents the mean squared displacement between neighboring points, V_{ki} is the i^{th} point in the k^{th} basis.

$$E_l(\bar{S},V)=\sum_i\sum_{j\in N(i)}((\left\|\bar{S}_i-\bar{S}_j\right\|-\delta)^2+\sum_k\left\|V_{ki}-V_{kj}\right\|^2) \tag{6}$$

Smoothness Consistency. We achieve smoothing by placing a cost on the variation of normal directions in a local neighborhood in the shape. The energy is formulated as:

$$E_n(S)=\sum_i\sum_{j\in N(i)}(1-\overrightarrow{N_i}\cdot\overrightarrow{N_j}) \tag{7}$$

The total energy is given in (8). α is the deformation parameter used to prevent unnaturally large deformations. We obtained our shape model $M=(\bar{S},V)$ by minimizing the total energy. The deformable 3D shape learnt is shown in Fig. 3.

$$E_{tot}(\bar{S},V,\alpha)=E_l(\bar{S},V)+\sum_i(E_{sc}^i+E_{kp}^i+E_n^i+\sum_k(\left\|\alpha_{ik}V_k\right\|_F^2)) \tag{8}$$

(a) mesh (b) model

Fig. 3. Deformable 3D models.

C. Deformation and detail extraction

1) DEFORMATION

After a deformable 3D model of is obtained, now given a new flower image, we are able to solve the deformation weights (initialized to 0) as well as all the camera projection parameters (scale, translation and rotation) by optimizing (9) to fixed $\bar{S}$,V. Note that we do not have access to annotated keypoints locations at this time, so the 'Keypoint Consistency' energy E_{kp} is ignored during the optimization. The objective function of reconstruction process and the definition of optimization process are shown in (9)-(10). Finally, because bas-relief has a lower height compared with 3D model, we compress the optimized model in a linear function. The compression rate in most relief generation algorithms is 0.02, so our experiment also uses 0.02 as compression rate.

$$E_r=E_{sc}+E_n \tag{9}$$

$$\min_{\alpha,\pi}\ E_r(S,\pi)+\delta(\pi,\pi_0)+\sum_k(\left\|\alpha_kV_k\right\|_F^2)\quad \text{subject to: } S=\bar{S}+\sum_k\alpha_kV_k \tag{10}$$

2) DETAIL EXTRACTION

The result of above optimization is a basic shape of the bas-relief, we still need to extract details from the image. Our method mainly calculates the depth of relief according to the gray values of the image. Firstly, image processing is used to enhance the details of the image, including gray image conversion, gradient information extraction and gamma correction. We enhance the contour edge by adding gradient information to the gray scale image. And gamma correction is used to improve the contrast of the image. As shown in (11)-(12), $g(I)$ and $\nabla(I)$ represent the gray scale image and gradient image respectively. Gamma correction uses different exponential parameters for different brightness levels to increase the slope of dark area of correction curve while keeping the slope of bright area of correction curve unchanged. Fig.4 shows the results of the process of image enhancement.

$$M_1=g(I)+\nabla(I) \tag{11}$$

$$gammaI=\begin{cases}M_1^{1/2.4}, 0\le M_1\le 90\\ M_1^{1/2.2}, 90\le M_1\le 255\end{cases} \tag{12}$$

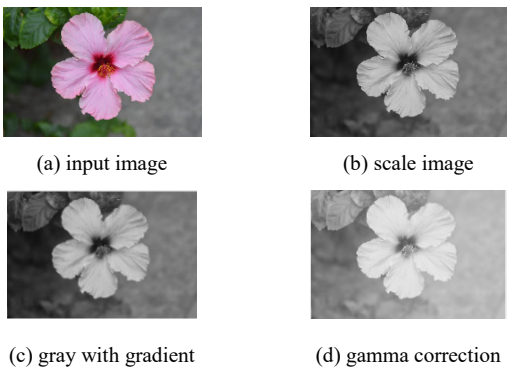

(a) input image (b) scale image

(c) gray with gradient (d) gamma correction

Fig. 4. The image enhancement process.

When only gray information can be obtained, we assume that the gray image is formed by light passing through the relief. With the reflection and refraction of light, different gray values are produced under the light at different thickness. According to the law of Illumination Intensity Reflection, the adjusted gray value $gammaI(x,y)$ is used to replace the reflection coefficient, (x,y) represents the coordinates of the pixels. The process is as follows (β and ρ are height factors. β is used to control the degree of compression in expression, and ρ is used to unify the values of details to $[0, \rho]$):

$$h_1(x,y) = \frac{\rho \sqrt{gammaI(x,y)+\beta}}{\sqrt{255+\beta}} \tag{13}$$

Similarly, according to the law of Illumination Intensity Projection, the complement of gray value is used to replace the reflection coefficient. The square root of the ratio of refractive index of two kinds of media is expressed by n. The refractive index of air is 1.0, and that of common materials is 1.5. Therefore, the square root of the ratio of the two media is approximated to 0.2. The process is as follows:

$$h_2(x,y) = \frac{\rho \times n\sqrt{255-gammaI(x,y)+\beta}}{\sqrt{255+\beta}} \tag{14}$$

Finally, we obtain the details of the relief by adding $h_1(x,y)$ and $h_2(x,y)$ [15]. Because vertices of the model are sparse, it is impossible to correspond with the extracted details. To solve this problem, we subdivide the model using loop sub-divisions to increase the number of vertices, filter the details to smooth them, and finally superimpose the details on the model to generate the final bas-relief.

IV. RESULTS AND ANALYSIS

In our experiment, we collected and labelled 171 flower images from the internet as our dataset. We generated bas-relief by setting different parameters β (β = 200, 500, 800) and ρ (ρ = 10, 20, 30). The experimental result shows that β = 500 and ρ = 20 can remain the edge smooth transition while retaining better details, as shown in Fig.5.

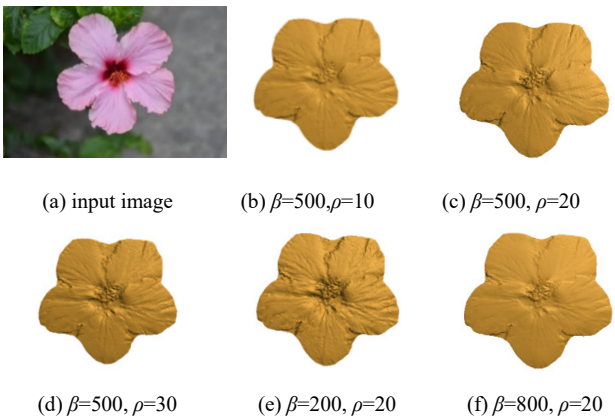

(a) input image (b) β=500,ρ=10 (c) β=500, ρ=20

(d) β=500, ρ=30 (e) β=200, ρ=20 (f) β=800, ρ=20

Fig. 5. Bas-reliefs generated using different height control parameters β and ρ.

We also compared our results with others'. One is Wang et al. [34], they generated the bas-relief with gradient option, which preserved the local features but missed the stamen or pistil of the flower (Fig.6(a)). Another is the method based on normal image of Wei et al. [2] achieved better contour, but without details on petals (Fig.6(b)). And our method preserved the details of both the stamen and petal(Fig.6(c)).

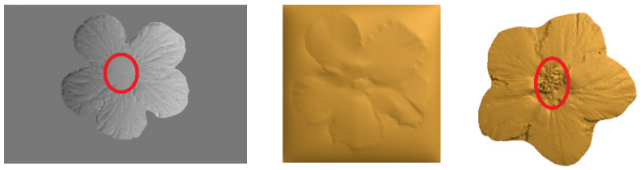

(a) Wang et al. [34] (b) Wei et al. [2] (c) Our result

Fig. 6. Compare with others'.

In addition, we separated the flower from the background. Fig.7 shows some experimental results with β = 500 and ρ = 20. It demonstrates that our method can generate bas-relief of flowers with various shapes and details, and can effectively extract details of petals. What's more, it is easily to extend to other types of flowers with more than five petals by adding and labelling keypoints of corresponding petals in the dataset. However, due to the simultaneous training of flowers with different petals, the bifurcation of five-petal flowers was not obvious, while the four-petal flowers tended to form five-petal flowers, resulting in a split on one petal (as shown in Fig.7(d), there is a split on the petal below). And because there are more front-view images in our dataset, the result of flower in the side view (Fig.7(b)) is not good as in the front view (Fig.7(a)). To solve it, we can try to balance the quantity of different views in our future work.

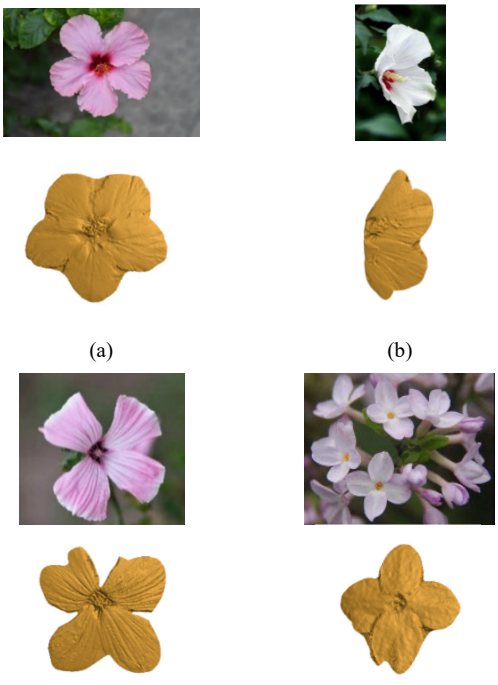

(a) (b)

(c) (d)

Fig. 7. Flower bas-reliefs.

In order to generate flower bas-reliefs as decorations, we drew the commonly used background images of bas-reliefs, and obtained relief models of the background by applying logarithmic transformation and triangulation on gray value. The experimental results were placed on the background to generate bas-reliefs as decorations similar to Fig.1. The results are shown in Fig.8.

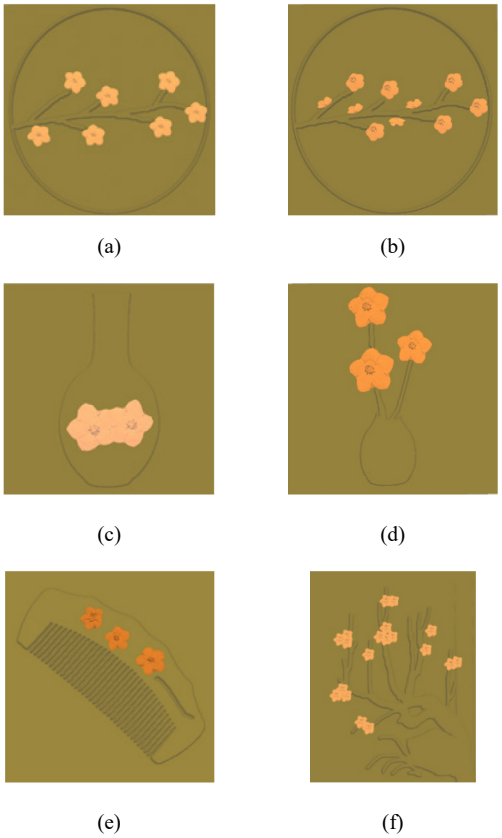

Fig. 8. Flower bas-reliefs as decorations.

In addition, we also carried out experiments on birds and clown fish. 132 images of birds were collected from the internet, and 12 keypoints ('leftEye', 'rightEye', 'beakBase', 'beakTip', 'lowerNeckBase', 'upperNeckBase', 'legCenter', 'wingBaseL', 'wingBaseR', wingTipL', 'wingTipR', 'tailTip') were designed. As for clown fish, we collected 151 images from the internet, and designed 10 keypoints ('eyeL', 'eyeR', 'mouse', 'pectoralFin', 'upperFin', 'lowerFin', 'analFin', 'tailFinTop', 'tailFinMiddle', 'tailFinDown'). Fig.9 shows some experimental results. Because the image set contained annotation information, the reconstruction results was not affected by complex background. Bas-reliefs of different birds and clown fish were reconstructed quite well, but the legs of bird were missing, as shown in Fig.9(a), because it was too slender compared with other parts.

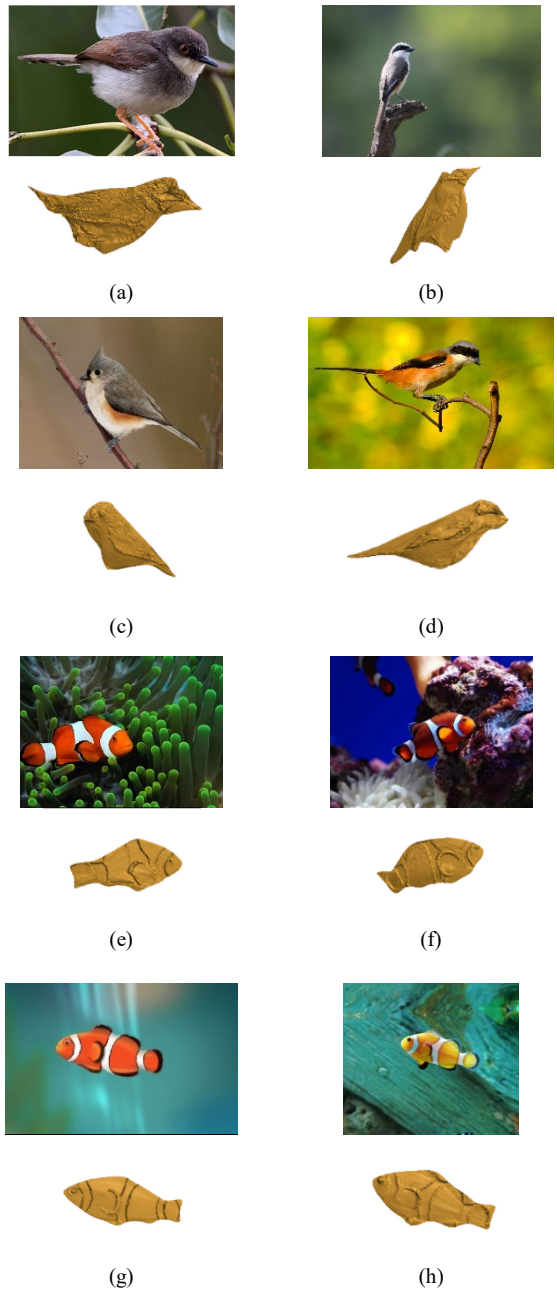

Fig. 9. Other results.

V. CONCLUSIONS AND FUTURE WORKS

Considering the convenience of using images as input in bas-reliefs generation is greater than using models and the similarity in objects of the same category, in this paper, we incorporate deformable 3D models into bas-reliefs generation and combine with detail extraction method to generate bas-relief flower models in different shapes. Our method also can be applied to other categories, such as birds and clown fish. Experimental results show that the flower bas-reliefs generated using our method can be applied to ornaments. However, this method needs to label datasets manually, and has problems with inaccurate reconstruction of some flowers. In the future work, we will consider automatically annotating and using the shape

information in details extracted to update the variant additionally to achieve better results.

ACKNOWLEDGMENT

This work was partially funded by Key Laboratory of Agricultural Internet of Things, Ministry of Agriculture and Rural Affairs, Yangling, Shaanxi 712100, China (2018AIOT-09), National Natural Science Foundation of China (61702433), Key Research and Development Program of Shaanxi Province (2018NY-127).

REFERENCES

[1] Y. W. Zhang, J. Wu, Z. P. Ji, M. Q. Wei and C. M. Zhang, "Computer-assisted Relief Modelling: A Comprehensive Survey," Computer Graphics Forum, vol. 38, no. 2, pp. 521-534, 2019.

[2] M. Wei, Y. Tian, W. M. Pang, C. Wang, M. Pang, and J. Wang, "Bas-relief modeling from normal layers," IEEE Transactions on Visualization and Computer Graphics, vol. 25, no. 4, pp. 1651-4665, 2019.

[3] M. Wang, L. Y. Yang, N. Geng, and D. He, "Survey and prospect of 3D model-based digital relief generation," Journal of Image and Graphics, vol. 23, no. 9, pp. 1273-1284, 2018.

[4] Q. Zeng, R. R. Martin, L. Wang, J. A. Quinn, Y. Sun, and C. Tu, "Region-based bas-relief generation from a single image," Graphical Models, vol. 76, no. 3, pp. 140-151, 2014.

[5] B. S. Sohn, "Ubiquitous creation of bas-relief surfaces with depth-of-field effects using smartphones," Sensors, vol. 17, no. 3, pp. 572-588. 2017.

[6] M. Dvorožňák, S. S. Nejad, O. Jamriška, A. Jacobson, L. Kavan, and D. Sýkora, "Seamless reconstruction of part-based high-relief models from hand-drawn images," Expressive, pp. 17-19, August. 2018.

[7] Q. Lu, L. Wang, X. Meng, and W. Wang, "The bas-relief generation method of human faces from 3D depth images and 2D intensity images," Journal of Computer-Aided Design and Computer Graphics vol. 27, no. 7, pp. 1172–1181, 2015.

[8] Z. Ji , W. Ma, and X. Sun, "Bas-relief modeling from normal images with intuitive styles," IEEE Transactions on Visualization and Computer Graphics, vol. 20, no. 5, pp. 675-685, 2014.

[9] Z. Ji, X. Sun, S. Li, and Y. Wang, "Real-time bas-relief generation from depth-and-normal maps on GPU," Computer Graphics Forum vol. 33, no. 5, pp. 75-83, 2014.

[10] Z. Ji, X. Sun, and W. Ma, "Normal image manipulation for bas-relief generation with hybrid styles,"unpublished.

[11] Y. Meng, M. Q. Zhou, W. Y. Shui, and Z. Wu, "Three-dimensional relief generation on freedom surface based on monocular image," Journal of System Simulation, vol. 27, no. 12, pp. 3012-3017, 2015.

[12] W. M. Wu, and L. G. Liu, "Course-to-fine bas-relief generation algorithm from images," College Mathematics, vol. 32, no. 12, pp. 1-7, 2016.

[13] S. Lee, and B. S. Sohn, "Generation of cartoon-style bas-reliefs from photographs," Multimedia Tools and Applications, no. 78, pp. 283811-284077, 2019.

[14] H. T. To, and B. S. Sohn, "Bas-relief generation from face photograph based on facial feature enhancement," Multimedia Tools and Applications, vol. 76, no. 8, pp. 10407-10423, 2017.

[15] Y. H. Zhu, B. Liu, and L. B. Zhang, "Algorithm and its implementation of bas-relief generation using image overlay," Journal of Huaqiao University(Natural Science), vol. 39, no. 3, pp. 172-178, 2018.

[16] Y. W. Zhang, Y. Chen, H. Liu, Z. Ji, and C. Zhang, "Modeling Chinese calligraphy reliefs from one image," Computers and Graphics, vol. 70, no. 7, pp. 300-306, 2017.

[17] Z. Li, S. Wang, J. Yu, and K. L. Ma, "Restoration of brick and stone relief from single rubbing images," IEEE Transactions on Visualization and Computer Graphics, vol. 18, no. 2, pp. 177-187, 2012.

[18] M. Kass, A. Witkin, and D. Terzopoulos, "Snakes: Active contour models," International Journal of Computer Vision, vol. 1, no. 4, pp. 321-331, 1988.

[19] D, Terzopoulos, M. Kass, and A. Witkin, "Constraints on deformable 3D models: Recovery 3D shape and non rigid motion," Artificial Intelligence, vol. 36, no. 1, pp. 91-123, 1988.

[20] L. M. Xia, S. W. Gu, and X. Q. Shen, "3D surface adaptive reconstruction based on deformable models," Journal of Image and Graphics, vol. 5, no. 5, pp. 396-400, 2018.

[21] L. F. Zhang, "A survey of image segmentation techniques using deformable models," Journal of Electronics and Information Technology, vol. 25, no. 3, pp. 395-403, 2003.

[22] Y. L. Hu, "3D face reconstruction based on the improved morphable model," Chinese Journal of Computers, vol. 28, no. 10, pp. 1671-1679, 2005.

[23] G. Shu, L. X. Yao, X. C. Yang, X. Zuo, and J. Yang, "3D facial caricaturing based on sparse morphable model," Acta Electronica Sinica, vol. 38, no. 8, pp. 1798-1802, 2010.

[24] M. Prasad, A. Fitzgibbon, A. Zisserman, and L. V. Gool, "Finding nemo: Deformable object class modelling using curve matching," IEEE Computer Society Conference on Computer Vision and Pattern Recognition, pp. 1-8, 2010.

[25] J. Hwang, S. Yu, J. Kim, and S. Lee, "3D face modeling using the multi-deformable method," Sensors, vol. 12, no. 12, pp. 12870-12889, 2012.

[26] S. Suwajanakorn, I. Kemelmacher-Shlizerman, and S. M. Seitz, "Total moving face reconstruction," Computer Vision, Springer International Publishing, pp. 796-812, 2014.

[27] A. Kar, Tulsiani S, Carreira, João, and J. Malik, "Category-specific object reconstruction from a single image," IEEE Conference on Computer Vision and Pattern Recognition, pp. 1-9, 2015.

[28] S. Vicente, J. Carreira, L. Agapito, and B. Jorge, "Reconstructing PASCAL VOC," IEEE Conference on Computer Vision and Pattern Recognition, pp. 1-8, 2014.

[29] A. W. Feng, D. Casas, and A, Shapiro. "Avatar reshaping and automatic rigging using a deformable 3D models," ACM SIGGRAPH Conference on Motion in Games, pp. 1-8, 2015.

[30] T. Weyrich, J. Deng, C. Barnes, and S. Rusinkiewicz, "Digital bas-relief from 3D scenes," ACM Transactions on Graphics, vol. 26, no. 3, 32, 2007.

[31] X. Sun, P. Rosin, R. Martin, and F. Langbein, "Bas-relief generation using adaptive histogram equalization," IEEE Transactions on Visualization and Computer Graphics, vol. 15, no. 4, pp. 642-653, 2009.

[32] L. Yang, C. Xiao, and J. Fang, "Multi-scale geometric detail enhancement for time-varying surfaces," Graphical Models, vol. 76, no. 5, pp. 413-425, 2014.

[33] J. L. Xu, C. N. Ling, G. Xu, Z. P. Ji and T. Rabczuk, "Spline bas-relief modeling from sketches by isogeometric analysis approach," Graphical Models, vol. 103, pp. 1-9. 2019.

[34] M. Wang, J. Chang, J. Pan, J. Zhang, "Image-based bas relief generation with gradient operation," Proceedings of the 11th IASTED International Conference Computer Graphics and Imaging, February 17-19, 2010.